# Distinct Unfolding and Refolding Pathways of Ribonuclease A Revealed by Heating and Cooling Temperature Jumps

Joan Torrent,* Stéphane Marchal,* Marc Ribó,† Maria Vilanova,† Cédric Georges,‡ Yves Dupont,‡§ and Reinhard Lange*

*Université Montpellier 2, UMR-S710, and INSERM Unit 710, Montpellier, France, and Ecole Pratique des Hautes Etudes, Paris, France; †Laboratori d'Enginyeria de Proteïnes, Departament de Biologia, Facultat de Ciències, Universitat de Girona, Girona, Spain; ‡Bio-Logic, Claix, France; and §Laboratoire de Biophysique moléculaire et cellulaire, Grenoble, France

ABSTRACT Heating and cooling temperature jumps (*T*-jumps) were performed using a newly developed technique to trigger unfolding and refolding of wild-type ribonuclease A and a tryptophan-containing variant (Y115W). From the linear Arrhenius plots of the microscopic folding and unfolding rate constants, activation enthalpy ($\Delta H^{\#}$), and activation entropy ($\Delta S^{\#}$) were determined to characterize the kinetic transition states (TS) for the unfolding and refolding reactions. The single TS of the wild-type protein was split into three for the Y115W variant. Two of these transition states, TS1 and TS2, characterize a slow kinetic phase, and one, TS3, a fast phase. Heating *T*-jumps induced protein unfolding via TS2 and TS3; cooling *T*-jumps induced refolding via TS1 and TS3. The observed speed of the fast phase increased at lower temperature, due to a strongly negative $\Delta H^{\#}$ of the folding-rate constant. The results are consistent with a path-dependent protein folding/unfolding mechanism. TS1 and TS2 are likely to reflect X-Pro$^{114}$ isomerization in the folded and unfolded protein, respectively, and TS3 the local conformational change of the $\beta$-hairpin comprising Trp$^{115}$. A very fast protein folding/unfolding phase appears to precede both processes. The path dependence of the observed kinetics is suggestive of a rugged energy protein folding funnel.

## INTRODUCTION

How do proteins morph into their folded, active forms? By which mechanisms do they unfold? Despite decades of computational and experimental research efforts, these processes remain elusive. To study folding and unfolding kinetics, proteins are usually forced into a nonequilibrium state by a rapid change of pressure, temperature, or concentration of chemical denaturant. The analysis of the relaxation kinetics toward the new equilibrium position can then inform about the reaction mechanism and the transition state (TS1) ensemble.

Most often, these processes are triggered by rapid flow techniques, involving turbulent mixing with high concentrations of a chemical denaturant, such as urea or guanidine hydrochloride. Such studies are generally confined to timescales of 1 ms or longer. An alternative technique is the laser-induced temperature jump (*T*-jump) (1–9). Although the *T*-jump is used much less often, it provides two main advantages: 1), it does not require the introduction of extraneous reagent into the sample; and 2), it permits the observation of conformational changes on the nanosecond timescale. However, these advantages are hampered by the inability to perform cooling jumps, and by the gradual temperature decrease in the system due to heat dissipation, which has already occurred after a few milliseconds. Obviously, many structural events occur on a much slower timescale. Therefore, an experimental technique is needed to initiate temperature-induced protein kinetics to study both the folding and unfolding reactions on timescales of 1 ms and longer. To achieve this goal, we have designed a new *T*-jump apparatus based on stopped-flow technology, hereafter called ''m*T*-jump'' (rapid-mixinig *T*-jump). The novel technical aspect of the experiments presented herein is that relaxation kinetics can be induced by heating as well as cooling *T*-jumps of magnitudes between 2 and 40°C. The possibility of studying protein folding/unfolding relaxation kinetics in both directions is important. Indeed, a number of recent findings from experimental and theoretical studies suggest that these processes are path-dependent, as a consequence of complex folding/unfolding energy landscapes (5,10–13).

We applied this technique to bovine pancreatic ribonuclease A (RNase A; EC 3.1.27.5). For many years, this enzyme has been a model for studies of protein structure, energetics, disulfide-bond reactions, and conformational folding (14–16). RNase A is a single domain protein that consists of 124 residues and possesses four disulfide bonds and four Pro residues, of which Pro$^{93}$ and Pro$^{114}$ are in the *cis* conformation (17). The *cis-trans* isomerization process of these Pro residues has been implicated in the heterogeneity of the conformational refolding and unfolding of RNase A (18).

As a consequence of the lack of Trp residues, the spectroscopic probes available for monitoring local conformational transitions of RNase A are limited. Therefore, in a previous study (19), we introduced a Trp residue on the solvent-exposed exterior of a C-terminal $\beta$-hairpin structure (17), which constitutes the main chain folding initiation site

*Submitted October 15, 2007, and accepted for publication December 21, 2007.*

Address reprint requests to Reinhard Lange, NSERM U710, CC 105, Université de Montpellier 2, Place Eugène Bataillon, F-34095 Montpellier cédex 5, France. Tel.: 33-467-14-33-85; Fax: 33-467-14-33-86; E-mail: lange@montp.inserm.fr.

Editor: Heinrich Roder.



0006-3495/08/05/4056/10 $2.00

doi: 10.1529/biophysj.107.123893

of the protein (20). In this work, we present the relaxation profiles obtained for the temperature-induced folding/unfolding of wild-type RNase A and its Y115W variant. The fluorescence change of the Trp variant is substantially enhanced upon unfolding, thereby reporting on the chain folding initiation site conformation as well as on the isomeric state of the neighboring X-Pro peptide bonds. This is the first time, at least under atmospheric pressure, that protein folding and unfolding kinetics has been investigated in both directions under identical physicochemical conditions.

## METHODS

### Materials

*Escherichia coli* strain BL21(DE3) used for the expression of RNase A was obtained from Novagen (Madison, WI). Oligonucleotides used for site-directed mutagenesis and molecular biology enzymes were from Roche (Basel, Switzerland). Other chemicals were from Sigma (St. Louis, MO).

### Protein expression and purification

Mutant and wild-type genes were expressed in BL21(DE3) cells using the T7 expression system, and the recombinant proteins were purified essentially as described by Torrent et al. (19). Protein concentrations were determined spectrophotometrically using a molar extinction coefficient at 278 nm of 9800 $M^{-1}$ $cm^{-1}$, and 14,800 $M^{-1}$ $cm^{-1}$, for the wild-type and variant protein, respectively (19).

### Equilibrium measurements

The heat-induced unfolding transitions of wild-type RNase A and Y115W variant were measured between 40 and 70°C by monitoring the change in fluorescence at 303 and 346 nm, respectively. The data were recorded in a 1-cm quartz cuvette on an Series 2 fluorescence-spectrophotometer (SLM Aminco, Amico Bowman, Foster City, CA) equipped with a thermostated sample holder. Lyophilized proteins were dissolved to a concentration of 0.1 mg $ml^{-1}$ in 50 mM sodium acetate buffer at pH 5.0, and filtered using a 0.22-mm filter. Fluorescence was excited at 278 nm (wild-type protein) and 290 nm (Y115W variant), using a bandwidth of 4 nm. Emission (accumulation of three scans) was collected between 280 and 430 nm for wild-type protein and between 310 and 440 nm for the Y115W variant, with a bandwidth of 8 nm. After each temperature increment/decrement, the protein was allowed to equilibrate before spectral recording. The equilibrium fluorescence intensity profiles versus temperature were fitted to Eq. 1,

$$X = \frac{(X_n - X_d) + (q - m)\,T}{1 + e^{-[(\Delta H - T\Delta S)/RT]}} + X_d + m\,T, \qquad (1)$$

where $X$ is the observed fluorescence intensity at temperature $T$, and $X_n$ and $X_d$ are the fluorescence intensities of the folded and unfolded states, respectively. $q$ and $m$ are correcting factors that take into account linear slopes of the pre- and posttransition regions, respectively.

### Kinetic measurements

Unfolding and refolding relaxation kinetics was measured by Tyr fluorescence excited at 278 nm for wild-type RNase A, and by Trp fluorescence excited at 290 nm for the Y115W variant. Final protein concentrations were 0.125 and 0.05 mg $ml^{-1}$, respectively, in 50 mM sodium acetate buffer at pH 5.0. The time-dependent fluorescence change was monitored by using a 295- or a 320-nm high-pass filter via a rapid-kinetics optical system MOS-200 from BioLogic (Grenoble, France). The rapid-mixing *T*-jump system (Fig. 1) is based on stopped-flow technology. The *T*-jump accessory was installed on a BioLogic (Grenoble, France) SFM-300 stopped-flow chassis. It has a temperature range from 5 to 90°C, precision of temperature reading of ±0.01°C, a maximum temperature jump of ±40°C, a temperature variation in the cuvette after a *T*-jump of <1%/30 s, and a maximum precision of *T*-jumps of ±0.1°C.

The device achieves temperature changes by mixing two solutions of initially different temperature. The final temperature of the mixture is determined by both the initial temperatures of the two solutions and the mixing ratio. In our stopped-flow experiments, 252 μl of solution were delivered at a mixing ratio of 1:1 to a high-density mixer via two thermostated syringes (*T* set at 25°C) and two storage lines mounted in thermostated aluminum blocks. The temperature of each line ($V = 150$ μl) was controlled by Peltier elements and monitored by thermocouples fixed to the corresponding block. Before each shot, the solutions in the storage lines were allowed to equilibrate for

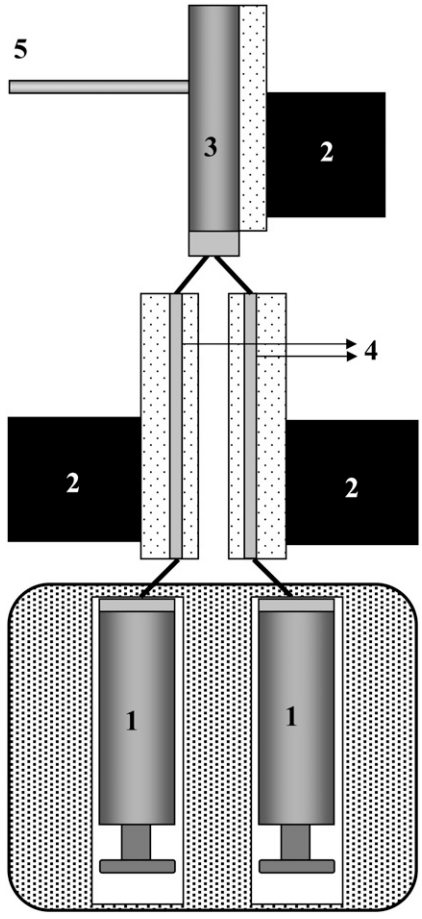


FIGURE 1 Schematic representation of the m*T*-jump apparatus. The instrument, installed on a Bio-Logic stopped-flow basis, is fully controlled by the manufacturer's software and achieves temperature changes by mixing two solutions of initially different temperatures, contained in two syringes (*1*). Three independent thermoelectric elements (*2*) are used to control the temperatures of the two storage lines (*4*) and of the observation cell (*3*). The storage lines are built into aluminum blocks in direct contact with the Peltier elements. Their volume is sufficient for one stopped-flow experiment. The temperature of the observation cell is monitored by a temperature probe (*5*) attached to its quartz surface.

3 min to ascertain homogenous and stable temperatures. The observation cuvette was temperature-regulated by a third Peltier element. Its temperature was adjusted to be equal to the temperature of the mix, as monitored on the quartz surface by a temperature probe. By using a total flow rate of 14 ml $s^{-1}$, a dead time of 3.7 ms was achieved.

## Temperature calibration

To adjust the temperature of the mix to that of the observation cell, calibration experiments were performed for each experimental *T*-jump condition, using *N*-acetyltryptophanamide as a temperature probe. The fluorescence of this fluorophore depends strongly on temperature; it decreases instantaneously when temperature increases, and vice versa, by ~1.4% for each degree Celsius. It was therefore suitable to monitor time-dependent temperature changes of the solution inside the observation cuvette resulting from a small temperature difference between the mix and the thermostated cuvette. Excitation was carried out at 250 nm, and the time-dependent fluorescence change was monitored using a 320 nm high-pass filter. For a typical calibration experiment, we mixed two solutions of *N*-acetyltryptophanamide at 6 $\mu$M under the precise experimental conditions (same temperature jump, mixing ratio, and flow rate) we intended to perform with the protein. If the system was well calibrated, no change in fluorescence was observed (the temperature of the mix was equal to the temperature of the cuvette). In contrast, a decreasing/increasing signal signified that the temperature of the mix increased/decreased in the cuvette during the experiment. Fine-tuning of the Peltier elements was repeated until a flat kinetic line was obtained.

## Determination of kinetic parameters from relaxation profiles

The relaxation profiles of the unfolding/folding reaction, after each *T*-jump (average of three jumps) were fitted to single or double (sequential) decays, using Bio-Kine software from BioLogic.

The individual rate constants $k_u$ and $k_f$ of the folding/unfolding reaction,

$$\text{Folded state} \underset{k_f}{\overset{k_u}{\rightleftharpoons}} \text{Unfolded state},$$

were determined according to Eqs. 2 and 3,

$$k_{obs} = k_u + k_f, \tag{2}$$

$$K_T = e^{-[\Delta G_{U_T}/RT]} = k_u/k_f, \tag{3}$$

where $T$ is the final temperature of each jump, $k_{obs}$ is the measured rate constant at temperature $T$, $K_T$ is the equilibrium constant at temperature $T$, and $\Delta G_{UT}$ is the free-energy change of unfolding obtained from equilibrium experiments at temperature $T$, determined from the fitted values of $\Delta H$ and $\Delta S$.

Using a two-state Kramers transition state analysis, the activation entropy $\Delta S^{\#}$ and activation enthalpy $\Delta H^{\#}$ of $k_u$ and $k_f$ were determined by fitting ln $k = f(1/T)$, according to Eq. 4,

$$\ln k = \ln(\nu_{(T1/2)}) + \ln(\eta_{(T1/2)}/\eta_{(T)}) + \Delta S^{\#}/R - (\Delta H^{\#}/R)(1/T), \tag{4}$$

where $\eta_{(T1/2)}$ and $\eta_{(T)}$ are the viscosity of water at the half-transition temperature and at the final experimental temperature, respectively. The preexponential factor $\nu_{(T1/2)}$ was set to $10^6$ $s^{-1}$. Alternatively, the Eyring formalism was used according to Eq. 5, where $k_B$ represents Boltzmann's constant, and $h$ Planck's constant.

$$\ln k = \ln(k_B/h) + (\Delta S^{\#}/R) - (\Delta H^{\#}/R)(1/T) + \ln T. \tag{5}$$

## RESULTS

### Folding and unfolding under equilibrium conditions

As shown in Fig. 2 *A*, high-temperature-induced unfolding of wild-type RNase A leads to a Tyr fluorescence increase of ~20%. For RNase Y115W, the fluorescence of the single Trp residue is quenched in the native state by local range interactions, particularly with disulfide bond 58–110. As shown in Fig. 2 *B*, high temperature disrupts these interactions and leads to a strong (sixfold) fluorescence enhancement. However, no significant shift of the fluorescence spectrum is observed, with a $\lambda_{max}$ between 342 and 344 nm, indicating a polar, water-exposed Trp environment already in the native state. The sigmoidal shape of the spectral transitions of wild-type and Y115W RNase A for both proteins indicates a two-state transition between native and unfolded states. The temperature at half transition, $T_{1/2}$, was 59.7°C for the wild-type and 56.4°C for the Trp variant, close to previously reported values (19,21,22). Also, the thermodynamic parameters

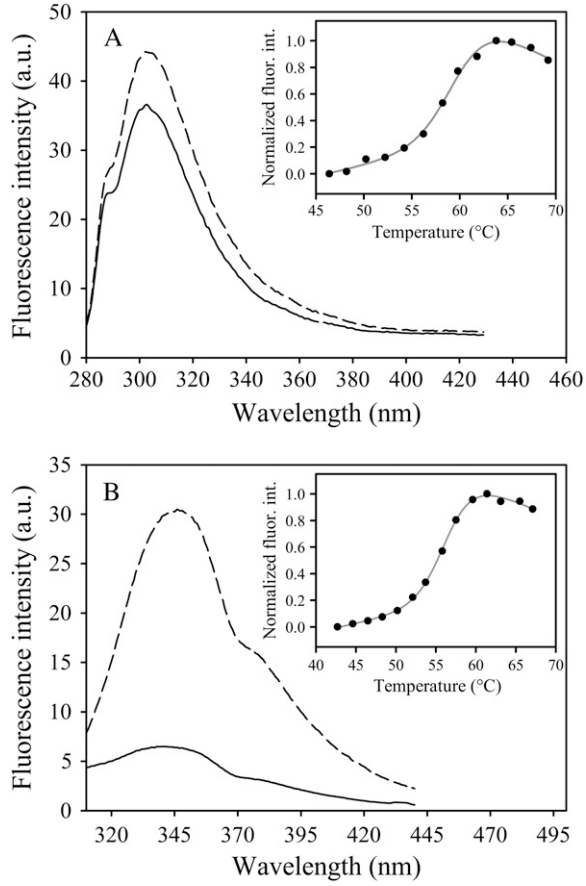


FIGURE 2 Fluorescence emission spectra and thermal transition curves of RNase A. (*A*) Wild-type protein. (*B*) Y115W variant. Spectra under native and unfolded conditions are represented as solid and dashed lines, respectively. Protein concentration was 0.1 mg $ml^{-1}$ in sodium acetate buffer, 50 mM, pH 5.0. (*Insets*) Temperature-induced unfolding curves. Solid lines are nonlinear least-squares fits based on a two-state model (Eq. 1).

deduced from the reversible transition (see Table 1) of Y115W were similar to those of the wild-type protein.

## Bi-directional *T*-jump induced kinetics

*T*-jumps were conducted in both directions over the whole range of the spectral transition. The *T*-jumps were of different magnitude, starting at the same temperature and reaching different final temperatures. Fig. 3, *A* and *B*, illustrates typical kinetic traces of Y115W observed after heating and cooling *T*-jumps. The kinetics resulted in significant fluorescence changes, matching the equilibrium measurements of Fig. 2. The kinetic traces for both heating and cooling *T*-jumps were monoexponential for wild-type and biexponential for Y115W RNase A. The amplitude of the rapid phase corresponded to ~20% of the total signal change.

The Arrhenius plots of $k_{obs}$, shown in Fig. 4, are composed on the left side (higher temperatures) of heating *T*-jump experiments, and on the right side (lower temperatures) of cooling *T*-jump experiments. Taken together, the Arrhenius plots appear to be bent upward. It is most striking that for Y115W, the upward curvature resulted in an acceleration of the fast phase at lower temperatures. For the wild-type protein, heating and cooling *T*-jumps appear to result in very similar rate constants. For the Y115W variant, small differences are observed for the $k_{obs}$ values recorded in heating and cooling *T*-jumps (Table 2).

## Independence of $k_{obs}$ on *T*-jump magnitude

How are these experiment-dependent differences in $k_{obs}$ values to be explained? Are the differences in $k_{obs}$ due to different directions of *T*-jump? Or are they due to different jump magnitude ($\Delta T$)? Indeed, in our experimental approach, the different final temperatures were reached by *T*-jumps of different magnitude, as the starting temperature was held constant for all jumps in one direction. To be able to choose between these two explanations, two other series of experiments were carried out, using the Y115W variant, with an inverse experimental set-up: we performed *T*-jumps of different magnitude starting from a different temperature and reaching the same final temperature. Again, biphasic kinetics was observed. The resulting $k_{obs}$ values are represented in Fig. 4 *B* in the open circles. As a matter of evidence, for heating *T*-jumps, the $k_{obs}$ values resulting from different jump magnitudes are all lying within the same two circles corresponding to the two kinetic phases. These circles coincide with the curved Arrhenius plot of $\ln(k_{obs})$ obtained by varying the final temperature (see above). Corresponding results were obtained for cooling *T*-jumps. Hence, we conclude that $k_{obs}$ depends on the direction of the *T*-jump, and not on its magnitude.

**TABLE 1 Thermodynamic parameters of wild-type RNase A and its Y115W variant calculated from temperature-induced unfolding curves at pH 5.0**

| Protein | $\Delta S$ (KJ mol$^{-1}$ K$^{-1}$)* | $\Delta H$ (KJ mol$^{-1}$)* | $T_{1/2}$ (°C)† | $\Delta G_{U40°C}$ (KJ mol$^{-1}$)† |
|---|---|---|---|---|
| Wild-type | 1.46 (0.29) | 484 (97) | 59.7 | 28.7 |
| Y115W | 1.53 (0.14) | 505 (47) | 56.4 | 25.2 |

Values in parentheses are the standard errors of the data.
*The change in entropy and enthalpy was calculated by fitting the equilibrium fluorescence intensity profiles to Eq. 1.
†The change in free energy was calculated using the fitted values $\Delta S$ and $\Delta H$.

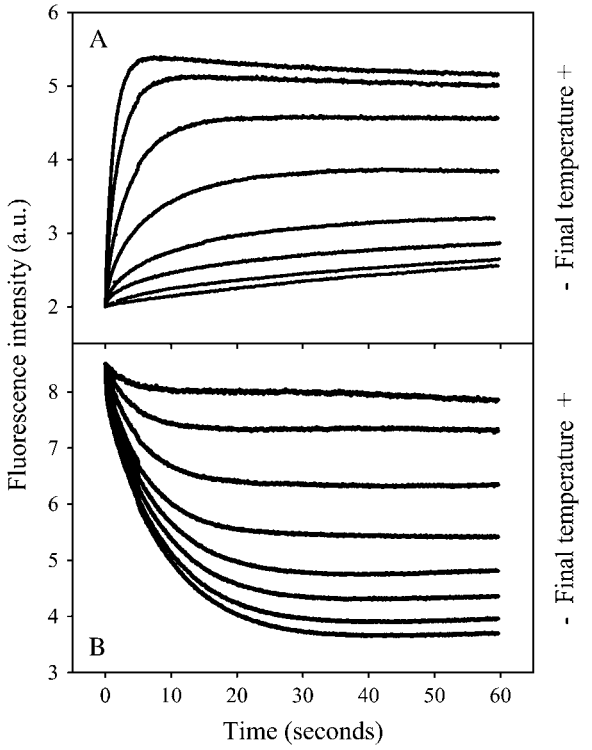


FIGURE 3 *T*-jump induced unfolding/folding relaxation kinetics of RNase A Y115W. (*A*) Heating *T*-jumps started from 45°C. They reached 49, 51, 53, 55, 57, 59, 61, and 63°C. (*B*) Cooling *T*-jumps started from 63°C. They reached 59, 57, 55, 53, 51, 49, 47, and 45°C. Solution conditions: Y115W at 0.05 mg ml$^{-1}$ in sodium acetate buffer, 50 mM, pH 5.0.

## Thermodynamic analysis

Understanding the above results is made possible by analyzing the properties of the microscopic folding and unfolding rate constants $k_f$ and $k_u$ of the reaction. As shown in Fig. 5, the Arrhenius plots of $k_f$ and $k_u$ were linear for both the single phase of the wild-type and the fast and slow phases of the variant protein. Hence, their thermodynamic activation parameters were determined by fitting $\ln k_f$ and $\ln k_u = f(1/T)$ to Eq. 4. The resulting kinetic activation parameters (Tables 3 and 4) were consistent with the corresponding thermodynamic parameters (Table 1), determined under equilibrium conditions. As a common feature, the slopes of $k_f = f(1/T)$ were close to zero or positive ($\Delta H^{\#} < 0$), and those of $k_u = f(1/T)$ were negative ($\Delta H^{\#} > 0$). Consistent with Eq. 3, their

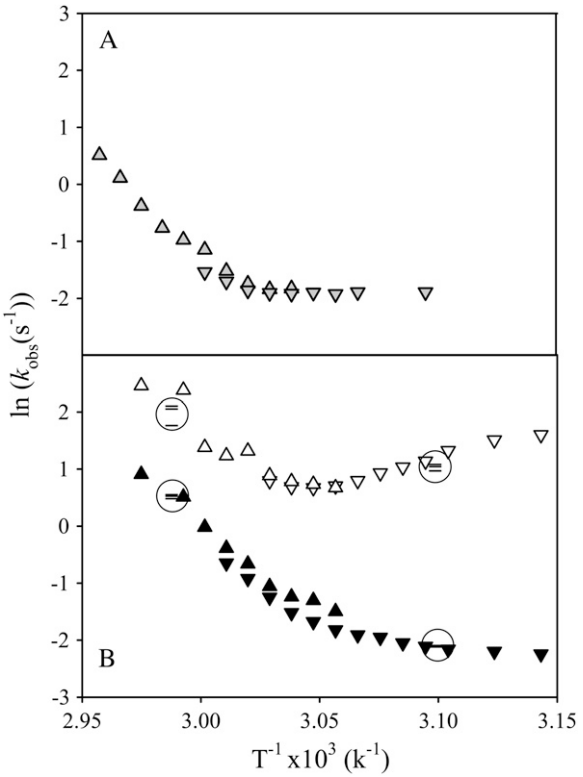


FIGURE 4 Temperature dependence of the measured rate constant ($k_{obs}$). $k_{obs}$ was determined from heating (*triangles*) and cooling (*inverted triangles*) *T*-jumps, for wild-type RNase A (*A*) and its Y115W variant (*B*). For the latter, a fast (*open triangles*) and a slow (*solid triangles*) kinetic phase were observed. $k_{obs}$ obtained from heating and cooling *T*-jumps of different magnitude (8, 15, and 22°C), but reaching the same final temperature, are represented as horizontal traits inside circles.

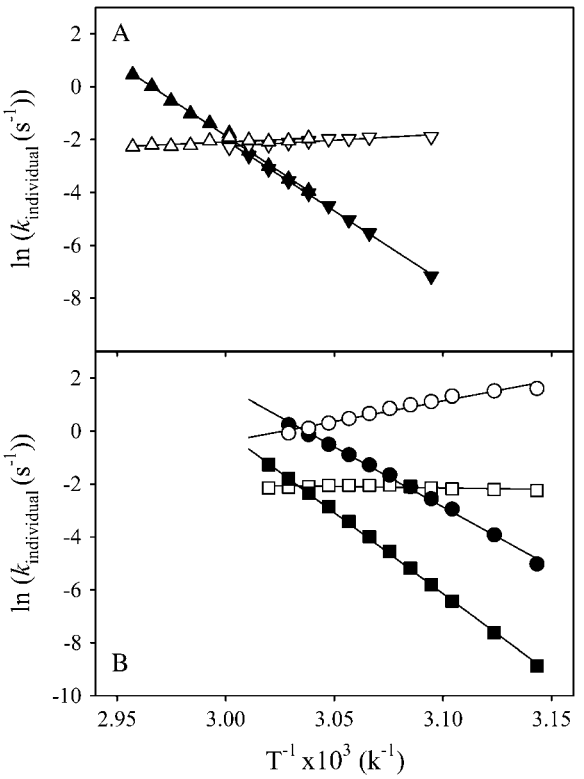


FIGURE 5 Temperature dependence of the individual rate constants ($k_f$, $k_u$). (*A*) $k_f$ (*open symbols*) and $k_u$ (*solid symbols*) determined from heating (*triangles*) and cooling (*inverted triangles*) *T*-jumps. The protein was wild-type RNase A. (*B*) $k_f$ (*open symbols*) and $k_u$ (*solid symbols*) for the fast (*circles*) and slow (*squares*) kinetic phases determined from cooling *T*-jumps. The protein was the RNase A variant Y115W.

crossing over took place at the half-transition temperature, $T_{1/2}$, where $K_T = 1$.

As shown in Fig. 5 and Tables 2 and 3, the kinetic parameters (individual rate constants as well as thermodynamic activation parameters) of wild-type RNase A did not significantly depend on the direction of the temperature jumps. In contrast, small but significant differences between the Arrhenius plots of $k_f$ and $k_u$ of the slow phase of Y115W variant were detected as a function of the direction of the *T*-jump (Fig. 6). The differences between heating and cooling *T*-jumps is also apparent when comparing the corresponding activation enthalpies, $\Delta H^{\#}$, and entropies, $\Delta S^{\#}$, in Table 4. For instance, the values of $\Delta H^{\#}$ of $k_f$ of the slow phase were $-72 \pm 8$ and $-5 \pm 4$ KJ mol$^{-1}$ in heating and cooling *T*-jumps, respectively.

**TABLE 2 Measured rate constants ($k_{obs}$) for the temperature-induced folding and unfolding reaction of wild-type RNase A and its Y115W variant at pH 5.0**

| | $k_{obs}$ ($s^{-1}$) at 56°C | |
|---|---|---|
| Protein | Heating *T*-jumps | Cooling *T*-jumps |
| Wild-type | 0.16 | 0.15 |
| Y115W* | 0.22/1.99 | 0.29/2.19 |

*The Y115W variant was observed in two kinetic phases.

## DISCUSSION

### Thermodynamic parameters of the kinetic transition state

The exponential character of all kinetic steps justified their analysis within transition state theory. The free energy barrier, $\Delta G^{\#}$, of a kinetic transition state contains an enthalpic ($\Delta H^{\#}$) and an entropic component ($\Delta S^{\#}$). Determining these components, especially $\Delta S^{\#}$, is dependent on the preexponential factor $\gamma$ in Eq. 6 (23). In the classical Eyring formalism (Eq. 5), $\gamma$ corresponds to $k_B T/h$. In the high-friction region of the Kramers formalism, $\gamma$ takes the form of a viscosity-corrected characteristic frequency, $\nu$, of diffusional motion over the energy barrier (Eq. 4) (24). For protein folding, depending on size and topology, different values of $\nu$ have been suggested, ranging from $0.1 \times 10^6$ to $50 \times 10^6$ $s^{-1}$ (25–28). Here, we used a $\nu$-value of $10^6$ $s^{-1}$ (1 $\mu s^{-1}$) which appears to be accepted as a reasonable consensus (29,30):

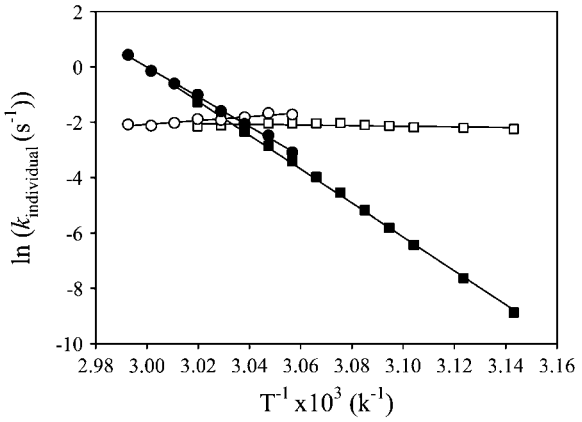


FIGURE 6 Path-dependent Arrhenius plots. $k_f$ (*open symbols*) and $k_u$ (*solid symbols*) were determined from heating (*circles*) and cooling (*squares*) *T*-jumps. The protein was the RNase A variant Y115W. Only the slow kinetic phase is shown.

$$k = \gamma \exp(-\Delta G^{\#}/RT) \tag{6}$$

The Kramers type analysis appears to be better suited for protein reactions in a viscous solvent than the Eyring formalism, which had been devised for chemical reactions in the gas phase. However, for the sake of comparability of the activation parameters reported here with data in the literature, we undertook in parallel an Eyring-type analysis. Although this affected the activation parameters only a little, as shown in Table 3, since $\gamma$ and $\Delta G^{\#}$ cannot be determined independently, the absolute values of $\Delta H^{\#}$ and $\Delta S^{\#}$ should be considered cautiously.

Another characteristic of the transition state is its heat capacity. However, the linearity of the Arrhenius plots indicated that the contribution of $\Delta C_p^{\#}$ could be neglected, at least in the limited temperature range (45–65°C) of our experiments. This is in contradiction to the reaction heat capacity, $\Delta C_p$, which had been determined by calorimetry as 5.3 KJ mol$^{-1}$ K$^{-1}$ (31), suggesting a nonzero value of $\Delta C_p^{\#}$. However, the introduction of $\Delta C_p^{\#}$ as an additional fitting parameter in Eq. 4 resulted in unreliable fitting results because of strong parameter dependencies. Therefore, in this analysis, an eventual contribution of $\Delta C_p^{\#}$ was not taken into account. Within the above-mentioned constraint, Fig. 7 offers a complete thermodynamic and kinetic description of the folding and unfolding of wild-type RNase A and its Y115W variant. As summarized in Table 3, heating and cooling *T*-jump-induced kinetics proceed by a common TS (identical $\Delta H^{\#}$ and $\Delta S^{\#}$ values) for the wild-type protein. For the Y115W variant, the energetic level of the TS is split into three distinct levels, as characterized by their activation enthalpies and entropies (Table 4). TS1 and TS2 occur after cooling (inducing folding) and heating (inducing unfolding) *T*-jumps, respectively. They reflect the slow kinetic phase. TS3 (of the fast phase) is identical in heating and cooling *T*-jumps. Hence, depending on the kinetic phase and the direction of the *T*-jump, the variant protein may adopt three different kinetic TS, distinguished by their activation enthalpy, $\Delta H^{\#}$, and activation entropy, $\Delta S^{\#}$. This suggests the existence of three different kinetic pathways.

**TABLE 3 Activation parameters for the temperature-induced folding and unfolding reaction of wild-type RNase A at pH 5.0**

| | Heating *T*-jumps | |
|---|---|---|
| $k_{individual}$ | $\Delta H^{\#}$ (KJ mol$^{-1}$) | $\Delta S^{\#}$ (KJ mol$^{-1}$ K$^{-1}$) |
| $k_f$ | −44 (8) | −0.27 (0.02) |
| | [−42 (5)] | [−0.39 (0.02)] |
| $k_u$ | 440 (8) | 1.19 (0.02) |
| | [442 (5)] | [1.07 (0.02)] |
| | Cooling *T*-jumps | |
| $k_{individual}$ | $\Delta H^{\#}$ (KJ mol$^{-1}$) | $\Delta S^{\#}$ (KJ mol$^{-1}$ K$^{-1}$) |
| $k_f$ | −53 (5) | −0.29 (0.01) |
| | [−33 (8)] | [−0.36 (0.02)] |
| $k_u$ | 431 (5) | 1.16 (0.01) |
| | [451 (8)] | [1.09 (0.02)] |

A viscosity corrected preexponential factor of $10^6$ s$^{-1}$ was used within the Kramers transition state formalism. Values enclosed in square brackets are calculated using the Eyring formalism. The standard errors of the data are indicated in parentheses.

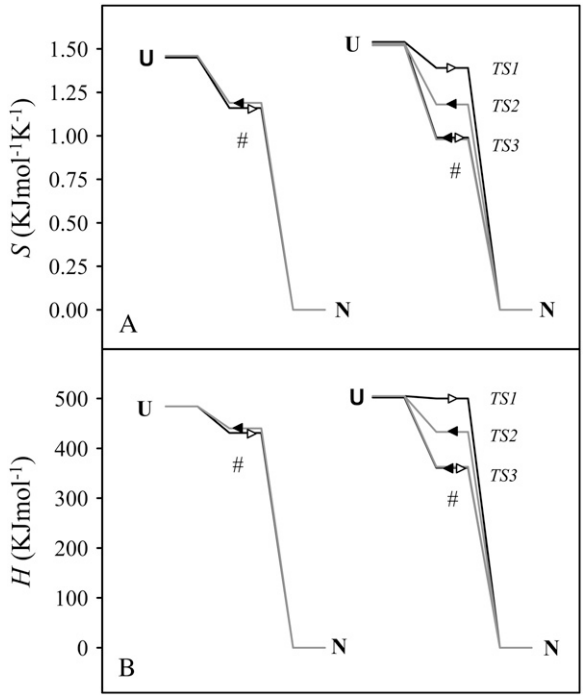


FIGURE 7 Kinetic transition states of the temperature-induced folding/unfolding reaction of RNase A. Changes of entropy (*A*) and enthalpy (*B*) were determined from the temperature dependence of $k_f$ and $k_u$ of both heating and cooling *T*-jumps of wild-type RNase A (*left*) and its Y115W variant (*right*). The direction of the *T*-jumps is indicated by arrows. Thermodynamic parameters of the folded state were set to zero. U and N denote the unfolded and native states, respectively. # represents the TS ensemble.

**TABLE 4 Activation parameters for the temperature-induced folding and unfolding reaction of RNase A Y115W at pH 5.0**

| | | Heating *T*-jumps | |
|---|---|---|---|
| | $k_{individual}$ | $\Delta H^{\#}$ (KJ mol$^{-1}$) | $\Delta S^{\#}$ (KJ mol$^{-1}$ K$^{-1}$) |
| TS3 | $k_f$ (fast) | −141 (13) | −0.54 (0.04) |
| | $k_u$ (fast) | 361 (13) | 0.98 (0.04) |
| TS2 | $k_f$ (slow) | −72 (8) | −0.35 (0.02) |
| | $k_u$ (slow) | 433 (8) | 1.18 (0.02) |
| | | Cooling *T*-jumps | |
| | $k_{individual}$ | $\Delta H^{\#}$ (KJ mol$^{-1}$) | $\Delta S^{\#}$ (KJ mol$^{-1}$ K$^{-1}$) |
| TS3 | $k_f$ (fast) | −142 (6) | −0.55 (0.02) |
| | $k_u$ (fast) | 363 (6) | 0.99 (0.02) |
| TS1 | $k_f$ (slow) | −5 (4) | −0.15 (0.01) |
| | $k_u$ (slow) | 500 (4) | 1.39 (0.01) |

A viscosity corrected pre-exponential factor of $10^6$ s$^{-1}$ was used within the Kramers transition state formalism. The standard errors of the data are indicated in parentheses.

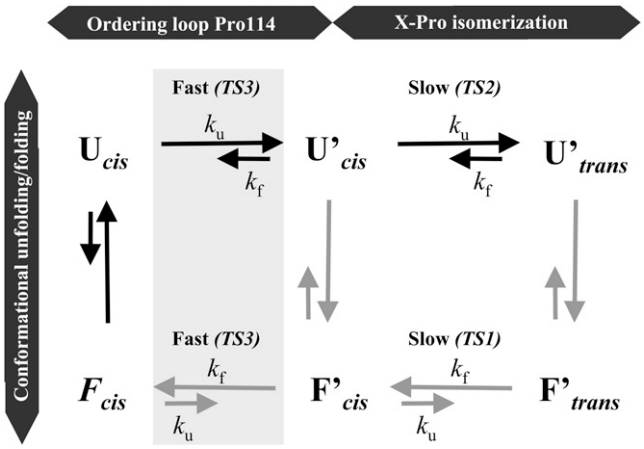


FIGURE 8 Kinetic reaction model for the temperature-triggered folding/unfolding of RNase A. The shaded area indicates the fast kinetic phases observed only for the Y115W variant. Solid and shaded arrows denote heating and cooling *T*-jumps, respectively. Undetectable kinetic phases corresponding to conformational unfolding/folding are denoted by the black vertical shape at left.

## Kinetic reaction model

On the basis of extensive stopped-flow studies (32–40), the following sequence of events has been described: 1), a fast phase monitoring purely conformational refolding/unfolding processes; and 2), several slower phases monitoring strictly local changes coupled to *cis-trans* isomerization of its three ''essential'' Pro residues (Pro$^{93}$, Pro$^{114}$, and Pro$^{117}$) (33). The fast folding/unfolding of the three-dimensional structure appears to be completed, under our experimental conditions of pH and temperature, within the dead time of the stopped-flow apparatus (3.7 ms). Indeed, the rate constant of this phase is 93 s$^{-1}$ at 20°C (41). Hence, because the isomeric state of the protein is essentially unchanging on the timescale of such a rapid cooperative unfolding/folding transition, we interpret our fluorescence-detected kinetics as the subsequent local changes in the environment of the Tyr (wild-type protein) or Trp (Y115W variant) residues, due to changes in the C-terminal $\beta$-hairpin structure of RNase A and *cis-trans* isomerization of the nearby X-Pro peptide bonds.

A possible reaction model is shown in Fig. 8. To explain the relaxation profiles obtained after heating *T*-jumps, we hypothesize the existence of one folded state, $F_{cis}$ (containing native X-Pro peptide groups), and three different states obtained after conformational unfolding, denoted $U_{cis}$, $U'_{cis}$, and $U'_{trans}$ containing the native (*cis*) or nonnative (*trans*) isomer. We use the symbol U′ to designate species arising after a local conformational change of the region around Pro$^{114}$. Stricto sensu, these states should not be considered as completely unfolded because thermal-unfolded RNase A retains some secondary structure (42–48). However, the residual structure in the unfolded state appears to be limited and of low stability. Therefore, and for simplicity, these states are denoted ''unfolded'' hereafter. Initially, at low temperature, all the protein (either wild-type protein or Y115W variant) is in state $F_{cis}$. The heating *T*-jump provokes the protein to relax in a very fast phase, not observed under our experimental conditions, from $F_{cis}$ to $U_{cis}$. The reaction proceeds further, allowing the protein to occupy first $U'_{cis}$, and subsequently $U'_{trans}$, with the former reaction ~7.5 times faster (at 56°C) than the latter. For wild-type protein, only the slow kinetic phase from $U'_{cis}$ to $U'_{trans}$ is observed.

In cooling *T*-jumps, most of the protein (~80–90%) is initially, at high temperature, in the $U'_{trans}$ state. A minor amount (~10–20%) is in state $U'_{cis}$. From each state, the protein relaxes in a very fast phase, not observed under our experimental conditions, to a folded state presenting the same X-Pro isomers as the corresponding unfolded state. Therefore, the folded states are denoted $F'_{trans}$ and $F'_{cis}$, respectively. The protein relaxes again from $F'_{trans}$ to $F'_{cis}$, and from $F'_{cis}$ to $F_{cis}$, giving rise to a major slow phase and a minor fast phase, respectively, with the former reaction ~9 times slower (at 56°C) than the latter. Again, for wild-type protein, only the slow phase from $F'_{trans}$ to $F'_{cis}$ is observed.

A plausible explanation for the biphasic relaxation profiles in the variant protein is that the sole Trp residue reports both on the local conformation of the loop around Pro$^{114}$ and on the isomeric state of this Pro residue. As a result, each process gives rise to an individual kinetic phase. It would have been interesting to shorten the incubation time in the storage lines (Fig. 1, *4*) before each shot to start mixing from differently populated isomeric species (such as in ''double jumps'' in the presence of chemical denaturants (35,38,49–51). However, this would require the development of a premixing *T*-jump device, which is beyond the scope of this work.

## Identity of the slow phase

The rate constants of the major slow phase observed for the Y115W variant (for the folding and unfolding reactions) are

similar to the monophasic relaxation kinetics we have observed for wild-type protein and, after correction for the corresponding temperature dependence of a given reaction, with those described in the literature. According to Juminaga et al. (37), this slow kinetics of the wild-type protein arises from $Tyr^{92}$ and $Tyr^{115}$ reporting on the *cis-trans* isomerization of $Pro^{93}$ and $Pro^{114}$, respectively. However, their respective contribution can be distinguished only by site-directed mutagenesis.

The transition states of the slow phase of the Y115W variant (TS1 and TS2) are different from that of the wild-type protein. Since $Trp^{115}$ reports on the isomerization state of $Pro^{114}$, rather than on that of $Pro^{93}$, this suggests that the activation parameters for the isomerization of $Pro^{114}$ under folding conditions are different from those observed under unfolding conditions. Such a particular behavior is in agreement with the unusual reduced activation energy of the X-$Pro^{114}$ peptide group under folding conditions (32), and extends the results previously reported by Cook et al. (52), who found, by an independent method, that Pro isomerization is speeded up under folding conditions and that a spectrally detectable folding intermediate at low temperatures (0–10°C) is present before Pro isomerization. It is likely that the quasinative intermediate described in this previous work, named $I_N$, corresponds to the $F'_{trans}$ species presenting nonnative (*trans*) isomers we observed after cooling *T*-jumps.

The fact that TS2 for the Y115W variant is identical to the TS of the wild-type protein indicates that under unfolding conditions, the activation parameters for the isomerization of $Pro^{114}$ are similar to those for isomerization of $Pro^{93}$. They are, however, dissimilar under folding conditions. Furthermore, in heating *T*-jumps, the value of $\Delta H^{\#}$ of $k_f$ of the slow phase was $-72 \pm 8$ KJ mol$^{-1}$ (within the constraint of $\nu = 10^6$ s$^{-1}$), rather similar to the activation energy at 25°C of prolyl isomerization, which has been determined as $-84$ KJ mol$^{-1}$ (53). These comparable values are a further argument in favor of the hypothesis that the slow phase reports on X-Pro isomerization.

## Identity of the fast phase

The fast processes for both heating and cooling *T*-jumps, with observed rate constants of $\sim 2$ s$^{-1}$ at 56°C, merely detected using the variant protein, are in fact slower than the global folding/unfolding processes (41), but much faster than the major slow phase ($\sim 0.2$–$0.3$ s$^{-1}$). We argue that they report on the local reorganization of the C-terminal $\beta$-hairpin of RNase A, which is stabilized mainly by highly hydrophobic interactions. This fast phase follows the global conformational unfolding/folding process.

Although it has been found previously that the reporting of $Tyr^{115}$ is very local, and that, accordingly, only the isomerization of X-$Pro^{114}$ is observed (18), the fast phase detected after replacement of $Tyr^{115}$ by Trp is comparable to the previously observed ''medium'' phase of refolding obtained from chemically induced unfolded RNase A (41). That phase may be assigned to a conformation in which both $Pro^{93}$ and $Pro^{114}$ are native *cis* and $Pro^{117}$ is nonnative *cis* (54). Thus, an alternative explanation can be proposed that receives further support by the analysis of the amplitude of the fast kinetic phase. The fact that this phase comprises $\sim$10–20% of the refolding/unfolding amplitude suggests that it reflects species that are only little populated, like those arising from a nonnative isomer of $Pro^{117}$ (18). A plausible explanation for the observation of such a phase in the variant protein can be proposed. Since $Pro^{117}$ is more distant from $Tyr^{115}$ than $Pro^{114}$, its isomerization signal is undersized in the wild-type protein and, consequently, may not be detectable. By contrast, the Y115W amino acid replacement makes readily apparent the contribution of $Pro^{117}$ isomerization through $Trp^{115}$.

## Acceleration of the folding rate at low temperature

The temperature dependence of $k_f$ of the fast phase, which accelerates when the temperature is lowered, is intriguing and seems to be in contradiction to the generally observed temperature dependence of kinetic rate constants of biochemical reactions. However, protein folding kinetics are more complex than ''ordinary'' biochemical reactions. Indeed, our results show clearly that this ''unusual'' behavior is due to a negative activation enthalpy. The overall energetic barrier of the activation free energy, $\Delta G^{\#}$, is maintained by a compensation of $\Delta H^{\#}$ with a strongly negative $T\Delta S^{\#}$ term. This entropic activation barrier for folding is consistent with studies of other proteins (55–57). The significant negative value of both activation parameters ($\Delta H^{\#}$ and $\Delta S^{\#}$) for the folding rate suggests that the TS remains hydrated while new intermolecular interactions are established. Moreover, it implies that the U-to-TS3 step is characterized by a reduction in chain entropy, suggesting a more ordered and structured activated complex compared to the U state. However, although the observation of a kinetic phase becoming faster at lower temperatures can be thermodynamically explained, it nevertheless calls for an understanding on the molecular level. As pointed out by Dobson (56), an explanation can be gleaned from theoretical studies, taking into account a rugged energy landscape (58). Indeed, Karplus (59) suggested, based on a cubic lattice model, that the protein folding rate at high temperature slows down, since the accessible configurational space increases and a longer search is needed to reach the TS. This situation seems to apply to $k_f$ of the fast phase. Accordingly, the cubic lattice model simulations constitute a further argument in favor of the fast phase reflecting a change in conformational order (the ordering of the C-terminal $\beta$-hairpin).

## Dissimilar folding and unfolding routes

This is, to our knowledge, the first report about protein relaxation kinetics induced by both heating and cooling

*T*-jumps. The thermodynamic activation parameters of the fast kinetic phase of Y115W variant (probably a conformational change of the C-terminal $\beta$-hairpin domain) are the same, whether determined by cooling or heating *T*-jumps. This path independence is also observed for the wild-type protein. This may be important information for researchers who do not have the capability to carry out *T*-jumps in both directions. However, the results of the slow kinetic phase of the Y115W variant, attributed to Pro isomerization, are intriguing, as they reveal a path dependence of the kinetics associated with protein folding and unfolding recent pressure-jump experiments had provided a first evidence of path-dependent RNase A unfolding (60). However, the high-pressure kinetic data do not seem to be directly comparable to the present results. This could indicate that pressure and temperature induce different folding/unfolding routes. Another type of path-dependent protein unfolding kinetics was previously discussed by Leeson et al., who used heating *T*-jumps of different amplitudes to induce unfolding of the major cold shock protein of *Escherichia coli* (5). The authors of this elegant article deplored the impossibility of carrying cooling *T*-jumps.

The ability to conduct cooling *T*-jumps is now made possible by the m*T*-jump technique. This novel technical achievement opens a whole field of possible investigations of protein relaxation kinetics in the folding direction, in the absence of chemical denaturants. The only other cooling jump device developed for studying biochemical reactions is the ''rapid-freeze'' apparatus (61). However, the latter technique does not allow the study of relaxation kinetics. Instead, it is used to stabilize reaction intermediates in view of their further structural analysis (62). The present path dependence of folding and unfolding relaxation kinetics induced by heating and cooling *T*-jumps may be considered as an experimental proof of a more than one-dimensional folding/unfolding energy surface. A further challenge will be to apply this new technical possibility to compare the folding and unfolding paths of other proteins.

The authors are grateful for the excellent technical assistance of M. C. Valentin, and for stimulating discussions with Dr. C. Balny. We are also indebted to Institut Fédératif de Recherche 122, Montpellier, France.

This work was carried out in the frame of COST Chemistry D30-WG005 cooperation and supported by a grant (BFU2006-15543-CO2-02/BMC) from the Ministerio de Educación y Ciencia (Spain).

## REFERENCES

1. Ballew, R. M., J. Sabelko, and M. Gruebele. 1996. Observation of distinct nanosecond and microsecond protein folding events. *Nat. Struct. Biol.* 3:923–926.
2. Callender, R. H., R. B. Dyer, R. Gilmanshin, and W. H. Woodruff. 1998. Fast events in protein folding: the time evolution of primary processes. *Annu. Rev. Phys. Chem.* 49:173–202.
3. Huang, C. Y., Z. Getahun, Y. Zhu, J. W. Klemke, W. F. DeGrado, and F. Gai. 2002. Helix formation via conformation diffusion search. *Proc. Natl. Acad. Sci. USA.* 99:2788–2793.
4. Kubelka, J., W. A. Eaton, and J. Hofrichter. 2003. Experimental tests of villin subdomain folding simulations. *J. Mol. Biol.* 329:625–630.
5. Leeson, D. T., F. Gai, H. M. Rodriguez, L. M. Gregoret, and R. B. Dyer. 2000. Protein folding and unfolding on a complex energy landscape. *Proc. Natl. Acad. Sci. USA.* 97:2527–2532.
6. Munoz, V., P. A. Thompson, J. Hofrichter, and W. A. Eaton. 1997. Folding dynamics and mechanism of $\beta$-hairpin formation. *Nature.* 390:196–199.
7. Phillips, C. M., Y. Mizutani, and R. M. Hochstrasser. 1995. Ultrafast thermally induced unfolding of RNase A. *Proc. Natl. Acad. Sci. USA.* 92:7292–7296.
8. Qiu, L., S. A. Pabit, A. E. Roitberg, and S. J. Hagen. 2002. Smaller and faster: the 20-residue Trp-cage protein folds in 4 micros. *J. Am. Chem. Soc.* 124:12952–12953.
9. Snow, C. D., L. Qiu, D. Du, F. Gai, S. J. Hagen, and V. S. Pande. 2004. Trp zipper folding kinetics by molecular dynamics and temperature-jump spectroscopy. *Proc. Natl. Acad. Sci. USA.* 101:4077–4082.
10. Chavez, L. L., S. Gosavi, P. A. Jennings, and J. N. Onuchic. 2006. Multiple routes lead to the native state in the energy landscape of the $\beta$-trefoil family. *Proc. Natl. Acad. Sci. USA.* 103:10254–10258.
11. Dill, K. A., and H. S. Chan. 1997. From Levinthal to pathways to funnels. *Nat. Struct. Biol.* 4:10–19.
12. Dinner, A. R., and M. Karplus. 1999. Is protein unfolding the reverse of protein folding? A lattice simulation analysis. *J. Mol. Biol.* 292:403–419.
13. Plotkin, S. S., and J. N. Onuchic. 2000. Investigation of routes and funnels in protein folding by free energy functional methods. *Proc. Natl. Acad. Sci. USA.* 97:6509–6514.
14. Neira, J. L., and M. Rico. 1997. Folding studies on ribonuclease A, a model protein. *Fold. Des.* 2:R1–R11.
15. Ribo, M., J. Font, A. Benito, J. Torrent, R. Lange, and M. Vilanova. 2006. Pressure as a tool to study protein-unfolding/refolding processes: the case of ribonuclease A. *Biochim. Biophys. Acta.* 1764:461–469.
16. Wedemeyer, W. J., E. Welker, M. Narayan, and H. A. Scheraga. 2000. Disulfide bonds and protein folding. *Biochemistry.* 39:4207–4216.
17. Wlodawer, A., L. A. Svensson, L. Sjolin, and G. L. Gilliland. 1988. Structure of phosphate-free ribonuclease A refined at 1.26 Å. *Biochemistry.* 27:2705–2717.
18. Wedemeyer, W. J., E. Welker, and H. A. Scheraga. 2002. Proline *cis-trans* isomerization and protein folding. *Biochemistry.* 41:14637–14644.
19. Torrent, J., J. P. Connelly, M. G. Coll, M. Ribo, R. Lange, and M. Vilanova. 1999. Pressure versus heat-induced unfolding of ribonuclease A: the case of hydrophobic interactions within a chain-folding initiation site. *Biochemistry.* 38:15952–15961.
20. Matheson, R. R., and H. A. Sheraga. 1978. Method for predicting nucleation sites for protein folding based on hydrophobic contacts. *Macromolecules.* 11:819–829.
21. Navon, A., V. Ittah, J. H. Laity, H. A. Scheraga, E. Haas, and E. E. Gussakovsky. 2001. Local and long-range interactions in the thermal unfolding transition of bovine pancreatic ribonuclease A. *Biochemistry.* 40:93–104.
22. Torrent, J., P. Rubens, M. Ribo, K. Heremans, and M. Vilanova. 2001. Pressure versus temperature unfolding of ribonuclease A: an FTIR spectroscopic characterization of 10 variants at the carboxy-terminal site. *Protein Sci.* 10:725–734.
23. Dragan, A. I., S. A. Potekhin, A. Sivolob, M. Lu, and P. L. Privalov. 2004. Kinetics and thermodynamics of the unfolding and refolding of the three-stranded $\alpha$-helical coiled coil, Lpp-56. *Biochemistry.* 43: 14891–14900.
24. Oliveberg, M., and P. G. Wolynes. 2005. The experimental survey of protein-folding energy landscapes. *Q. Rev. Biophys.* 38:245–288.
25. Jager, M., H. Nguyen, M. Dendle, M. Gruebele, and J. W. Kelly. 2007. Influence of hPin1 WW N-terminal domain boundaries on function, protein stability, and folding. *Protein Sci.* 16:1495–1501.
26. Ma, H., and M. Gruebele. 2005. Kinetics are probe-dependent during downhill folding of an engineered $\lambda$6-85 protein. *Proc. Natl. Acad. Sci. USA.* 102:2283–2287.

27. Naganathan, A. N., U. Doshi, A. Fung, M. Sadqi, and V. Munoz. 2006. Dynamics, energetics, and structure in protein folding. *Biochemistry.* 45:8466–8475.

28. Nguyen, H., M. Jager, J. W. Kelly, and M. Gruebele. 2005. Engineering a $\beta$-sheet protein toward the folding speed limit. *J. Phys. Chem. B.* 109:15182–15186.

29. Munoz, V. 2007. Conformational dynamics and ensembles in protein folding. *Annu. Rev. Biophys. Biomol. Struct.* 36:395–412.

30. Zhu, Y., D. O. Alonso, K. Maki, C. Y. Huang, S. J. Lahr, V. Daggett, H. Roder, W. F. DeGrado, and F. Gai. 2003. Ultrafast folding of $\alpha$3D: a de novo designed three-helix bundle protein. *Proc. Natl. Acad. Sci. USA.* 100:15486–15491.

31. Makhatadze, G. I., and P. L. Privalov. 1995. Energetics of protein structure. *Adv. Protein Chem.* 47:307–425.

32. Bhat, R., W. J. Wedemeyer, and H. A. Scheraga. 2003. Proline isomerization in bovine pancreatic ribonuclease A. 2. Folding conditions. *Biochemistry.* 42:5722–5728.

33. Dodge, R. W., and H. A. Scheraga. 1996. Folding and unfolding kinetics of the proline-to-alanine mutants of bovine pancreatic ribonuclease A. *Biochemistry.* 35:1548–1559.

34. Garel, J. R., B. T. Nall, and R. L. Baldwin. 1976. Guanidine-unfolded state of ribonuclease A contains both fast- and slow-refolding species. *Proc. Natl. Acad. Sci. USA.* 73:1853–1857.

35. Houry, W. A., D. M. Rothwarf, and H. A. Scheraga. 1994. A very fast phase in the refolding of disulfide-intact ribonuclease A: implications for the refolding and unfolding pathways. *Biochemistry.* 33:2516–2530.

36. Juminaga, D., W. J. Wedemeyer, R. Garduno-Juarez, M. A. McDonald, and H. A. Scheraga. 1997. Tyrosyl interactions in the folding and unfolding of bovine pancreatic ribonuclease A: a study of tyrosine-to-phenylalanine mutants. *Biochemistry.* 36:10131–10145.

37. Juminaga, D., W. J. Wedemeyer, and H. A. Scheraga. 1998. Proline isomerization in bovine pancreatic ribonuclease A. 1. Unfolding conditions. *Biochemistry.* 37:11614–11620.

38. Sendak, R. A., D. M. Rothwarf, W. J. Wedemeyer, W. A. Houry, and H. A. Scheraga. 1996. Kinetic and thermodynamic studies of the folding/unfolding of a tryptophan-containing mutant of ribonuclease A. *Biochemistry.* 35:12978–12992.

39. Udgaonkar, J. B., and R. L. Baldwin. 1995. Nature of the early folding intermediate of ribonuclease A. *Biochemistry.* 34:4088–4096.

40. Welker, E., K. Maki, M. C. Shastry, D. Juminaga, R. Bhat, H. A. Scheraga, and H. Roder. 2004. Ultrarapid mixing experiments shed new light on the characteristics of the initial conformational ensemble during the folding of ribonuclease A. *Proc. Natl. Acad. Sci. USA.* 101:17681–17686.

41. Kimura, T., S. Akiyama, T. Uzawa, K. Ishimori, I. Morishima, T. Fujisawa, and S. Takahashi. 2005. Specifically collapsed intermediate in the early stage of the folding of ribonuclease A. *J. Mol. Biol.* 350: 349–362.

42. Benz, F. W., and G. C. Roberts. 1975. Nucler magnetic resonance studies of the unfolding of pancreatic ribonuclease. *J. Mol. Biol.* 91: 345–365.

43. Chen, M. C., and R. C. Lord. 1976. Laser Raman spectroscopic studies of the thermal unfolding of ribonuclease A. *Biochemistry.* 15:1889–1897.

44. Denisov, V. P., and B. Halle. 1998. Thermal denaturation of ribonuclease A characterized by water 17O and 2H magnetic relaxation dispersion. *Biochemistry.* 37:9595–9604.

45. Labhardt, A. M. 1982. Secondary structure in ribonuclease. I. Equilibrium folding transitions seen by amide circular dichroism. *J. Mol. Biol.* 157:331–355.

46. Matthews, C. R., and D. G. Westmoreland. 1975. Nuclear magnetic resonance studies of residual structure in thermally unfolded ribonuclease A. *Biochemistry.* 14:4532–4538.

47. Seshadri, S., K. A. Oberg, and A. L. Fink. 1994. Thermally denatured ribonuclease A retains secondary structure as shown by FTIR. *Biochemistry.* 33:1351–1355.

48. Sosnick, T. R., and J. Trewhella. 1992. Denatured states of ribonuclease A have compact dimensions and residual secondary structure. *Biochemistry.* 31:8329–8335.

49. Houry, W. A., D. M. Rothwarf, and H. A. Scheraga. 1995. The nature of the initial step in the conformational folding of disulphide-intact ribonuclease A. *Nat. Struct. Biol.* 2:495–503.

50. Houry, W. A., D. M. Rothwarf, and H. A. Scheraga. 1996. Circular dichroism evidence for the presence of burst-phase intermediates on the conformational folding pathway of ribonuclease A. *Biochemistry.* 35:10125–10133.

51. Houry, W. A., and H. A. Scheraga. 1996. Structure of a hydrophobically collapsed intermediate on the conformational folding pathway of ribonuclease A probed by hydrogen-deuterium exchange. *Biochemistry.* 35:11734–11746.

52. Cook, K. H., F. X. Schmid, and R. L. Baldwin. 1979. Role of proline isomerization in folding of ribonuclease A at low temperatures. *Proc. Natl. Acad. Sci. USA.* 76:6157–6161.

53. Balbach, J., and F. X. Schmid. 2000. Proline isomerization and its catalysis in protein folding. *In* Mechanism of protein folding, 2nd ed. R. H. Pain, editor. Oxford University Press, New York. 212–249.

54. Scheraga, H. A., W. J. Wedemeyer, and E. Welker. 2001. Bovine pancreatic ribonuclease A: oxidative and conformational folding studies. *Methods Enzymol.* 341:189–221.

55. Choy, W. Y., Z. Zhou, Y. Bai, and L. E. Kay. 2005. An 15N NMR spin relaxation dispersion study of the folding of a pair of engineered mutants of apocytochrome b562. *J. Am. Chem. Soc.* 127:5066–5072.

56. Matagne, A., M. Jamin, E. W. Chung, C. V. Robinson, S. E. Radford, and C. M. Dobson. 2000. Thermal unfolding of an intermediate is associated with non-Arrhenius kinetics in the folding of hen lysozyme. *J. Mol. Biol.* 297:193–210.

57. Oliveberg, M., Y. J. Tan, and A. R. Fersht. 1995. Negative activation enthalpies in the kinetics of protein folding. *Proc. Natl. Acad. Sci. USA.* 92:8926–8929.

58. Bryngelson, J. D., J. N. Onuchic, N. D. Socci, and P. G. Wolynes. 1995. Funnels, pathways, and the energy landscape of protein folding: a synthesis. *Proteins.* 21:167–195.

59. Karplus, M., and A. Sali. 1995. Theoretical studies of protein folding and unfolding. *Curr. Opin. Struct. Biol.* 5:58–73.

60. Font, J., J. Torrent, M. Ribo, D. V. Laurents, C. Balny, M. Vilanova, and R. Lange. 2006. Pressure-jump-induced kinetics reveals a hydration dependent folding/unfolding mechanism of ribonuclease A. *Biophys. J.* 91:2264–2274.

61. Bray, R. C. 1961. Sudden freezing as a technique for the study of rapid reactions. *Biochem. J.* 81:189–193.

62. Cherepanov, A. V., and S. De Vries. 2004. Microsecond freeze-hyperquenching: development of a new ultrafast micro-mixing and sampling technology and application to enzyme catalysis. *Biochim. Biophys. Acta.* 1656:1–31.